Supplemental Online Material Accompanying:

Comparing *S. pombe* and *S. cerevisiae* Genetic Interactions Reveals Functional Repurposing and Identifies New Organelle Homeostasis and Mitosis Control Genes

Adam Frost[1*], Marc G. Elgort[1], Onn Brandman[2,3,4], Clinton Ives[2,3,4], Sean R. Collins[7], Lakshmi Miller-Vedam[2,3,4], Jimena Weibezahn[2,3,4], Marco Y. Hein[5], Ina Poser[6], Matthias Mann[5], Anthony A. Hyman[6], and Jonathan S. Weissman[2,3,4]

1. Department of Biochemistry and Huntsman Cancer Institute, University of Utah, School of Medicine, Salt Lake City, UT 84112
2. Department of Cellular and Molecular Pharmacology, and
3. California Institute for Quantitative Biomedical Research, and
4. Howard Hughes Medical Institute, University of California, San Francisco, CA 94158
5. Proteomics and Signal Transduction, Max-Planck Institute of Biochemistry, Martinsried, Germany
6. Max Planck Institute of Molecular Cell Biology and Genetics, 01307 Dresden, Germany
7. Department of Chemical and Systems Biology, Stanford University, 318 Campus Drive, Clark Building W2.1, Stanford, CA 94305-5174, USA

*to whom correspondence should be addressed (frost@biochem.utah.edu)

SUPPLEMENTAL TABLE AND FIGURE LEGENDS

Supplemental Table 1

Amino acid alignments statistics for outlier examples of correlated pairwise relationships observed in both budding and fission yeast (**green**), in budding yeast but not fission yeast (**blue**), and in fission yeast but not in budding yeast (**red**). Divergent relationships that were tested in directed assays are in **bold** text. For apparent orthologs (reciprocal best-match BLAST scores (Altschul, *et al.* 1997)), amino acid alignments statistics are listed and reported graphically in Figure 2D. Higher max scores, percent identities, and smaller Expect scores (number of times that an unrelated sequence would obtain a score S higher by chance) indicate greater degrees of conservation, while higher percent coverage indicates whether one ortholog contains additional sequence features that are not found in the other. Orthologs that share the same genetic relationships have similar BLAST scores, percent identities and Expect scores, but tend to have higher percent coverages. Two reported orthologs show such poor conservation—Apq12 and Atg14—they may not be true functional orthologs.

Supplemental Figure 1: Strain Generation and Crosses

(A) Schematic overview of the fusion PCR protocol used to generate knockout cassettes. The NATMX4/6 marker was amplified using non-palindromic and unique GC-rich flanking sequence. 350-500 bp amplicons were generated 5' (P2 and P3) and 3' (P4 and P5) to the targeted ORF using the cognate GC-rich sequences fused to P3 and P4 oligonucleotides. A second stage annealing at 70°C followed by amplification of the fused cassette with P2 and P5 oligonucleotides generated the complete targeting cassette. All PCR steps were performed in 96 well format and the final products were isolated and concentrated on MinElute 96-well PCR purification plates (Qiagen, 28053). Correction recombination events were verified in two stages, 1) failure to amplify the central 200-300 bp of the

targeted ORF and 2) successful amplification of the insertion site sequence using primers P1 and P6 paired with oligos within the NATMX4/6 cassette. **(B)** Propagation, crosses, and selection of double mutants were all performed as described in 32x48 format. Final double mutant plates were scanned on an Epson PhotoPerfection 350 scanner to minimize barrel distortion.

Supplemental Figure 2: Colony size and Linkage Disequilibrium Analysis

(A) After scanning, the integrated intensity of each colony was extracted using an algorithm implemented in MATLAB (available upon request). A small window of a scanned plate indicating two synthetic lethal colonies (red arrows) and **(B)** a corresponding 3D representation following integrated intensity extraction. **(C)** Scatter plot of biological and technical replicates of normalized colony sizes where the x- and y- axes correspond to two replicates and the color of the data point corresponds to a third (blue low, red high). Every double mutant was made via biological and technical triplicates per patch and in a second triplicate batch 6-12 months later. **(D)** Scatter plot (blue) of raw S-scores (y-axis) for double mutants on the same chromosome separated by base pairs from the query gene locus (x-axis). Contaminated or otherwise unlinked strains were excluded from subsequent analysis. As described previously (Roguev *et al*, 2008), linkage disequilibrium in *S. pombe* is apparent globally at 500kb in either direction of the query locus (red), but varies in magnitude per locus. **(E)** Line plot of apparent S-score per position along the three chromosomes, revealing linkage disequilibrium for the query locus on chromosome 1 (red line). For loci with smooth linkage-based decrements in apparent S-score due to limiting spore numbers, S-scores for double mutants between ~300kb and ~1000kb were normalized (green line) after modeling the linkage-based decay (black line). S-scores for double mutants closer than 300kb to the target locus were rejected uniformly.

Supplemental Figure 3: Global View of the *S. pombe* Genetic Interaction Map

Hierarchical clustering of genetic interaction profiles. A full "clustergram" for 597x1295 matrix of S-

scores (available online for download as supplemental database or through a searchable web-based interface at http:www.YeastQuantitativeGenetics.org). Aggravating interactions are scored as negative S-scores and color-coded with blue pixels. Ameliorating interactions are scored as positive S-scores and color-coded with yellow pixels. Black pixels correspond to fitness measurements that match the expected fitness (no genetic interaction). Grey pixels correspond to missing data for double mutants that could not be generated or that had to be excluded due to linkage disequilibrium artifacts (see Figure S2). Two clusters not referred to in the main text are boxed in red and viewed as enlargements as illustrations of the power of this method to identify complexes and functional connections.

Supplemental Figure 4: VPS4 and SNF7 deletions strains do not alter spindle pole body duplication or fragmentation in *S. cerevisiae*

(A) Cartoon representation of the budding yeast spindle pole body based on (Bullitt *et al*., 1997). C-terminal GFP tagged strains for components in each principal layer were analyzed for duplication or fragmentation abnormalities after deletion of **(B)** *VPS4* and **(C)** *SNF7*. A minimum of 500 cells per genotype per isolate (4 isolates, 2000 cells total) per deletion were examined. Note the enlarged vacuoles as expected for Δ*VPS4* and Δ*SNF7* cells.

Supplemental Figure 5: Phylogenetic analysis of Far3p and Far7p

(A) Phylogenetic tree of select ascomycota adapted from Fitzpatrick et al. (2006), Dujon et al. (2004), and Gordon et al. (2009). Species that posses apparent orthologs of Far3p and Far7p are indicated, with **(B)** top scoring amino acid sequences recovered from BLASTP, PSI-BLAST and PHI-BLAST searches of all non-redundant GenBank coding sequences (Altschul, *et al.* 1997).

Supplemental Figure 6: STRIPAK Signaling Complexes Bridge the Nuclear Envelope, Centrosomes and the Golgi

(A) *far8*/STRN3, *far10*/SLMAP, *far11*/STRIP1 and *mob1*/MOBKL3 transcript abundance following siRNA transfection of HeLa cells by quantitative PCR. Transcript abundance was normalized to the abundance of the mRNA for a ribosomal subunit, RPL19 (see Methods). A Western blot against far10/SLMAP after silencing with two different duplexes versus control (siLuciferase) transfected cells shown as an inset. **(B)** Maximum intensity Z-projections of fluorescence micrographs of a representative HeLa cell that has been depleted of STRIP1 for 48 hours. Fluorescence staining shows Golgi (red, anti-Giantin), the Golgi-localized STRN3 (green, STRN3-eGFP), and nuclei (blue, DAPI). **(C)** Maximum intensity Z-projections of fluorescence micrographs of HeLa cells depleted of STRN3 for 48 hours. Fluorescence staining reveals the same horeshoe and torus-shaped nuclei see after depletion of STRIP1. **(D)** Maximum intensity Z-projections of fluorescence micrographs of HeLa cells depleted of MOBKL3 for 30 hours. The accumulation of abnormal mitotic cells after siMOBKL3 leads to massive cell death by 48 hours. Mitotic cells uniformly reveal abnormal spindles and failures of chromosome condensation. **(E)** Maximum intensity Z-projections of fluorescence micrographs of control HeLa cells expressing full-length mCherry-SLMAP for <24 hours and stained for Golgi (green, Giantin), and DNA (blue, DAPI). mCherry-SLMAP localizes to the outer-nuclear envelope and some perinuclear ER structures, but does not localize to the Golgi.

SUPPLEMENTAL DATSETS

Java Treeview-formatted files (.cdt, .gtr, .jv. and .pcl) generated by Cluster 3.0 (Eisen *et al.* 1998, de Hoon *et al.*, 2004). The columns of the matrix correspond to the genetic interaction profiles of the Query *h*-, NAT-marked query strains. The rows of the matrix correspond to the genetic interaction profiles of Array *h*+, KAN-marked array strains. The names of the row and columns are formatted as follows: GeneID_genename_Description_(budding yeast ortholog in upper case). Some rows are labeled "LINKED_PROFILE_near_*locus.*" These profiles were generated for array strains that proved upon linkage analysis to have excellent reproducibility but to be linked to a locus other than the locus annotated by BIONEER—suggesting mis-annotation. The resolution of our linkage analysis is not fine enough to identify the true locus, but we have listed the most tightly linked locus. Two versions of the cluster maps are included. In the first, "Frost_Spombe_GI_Unaveraged", the S-scores along the diagonal of the matrix, corresponding to double mutants generated by reciprocal crosses, have not been averaged due to potential confounding differences in the strain backgrounds. In the second, "Frost_Spombe_GI_Diagonal_Averaged," S-scores corresponding to double mutants generated by reciprocal crosses have been averaged.

EXPERIMENTAL PROCEDURES

Strains and Genetic Crosses

For the fission yeast Genetic Interaction map the array G418 (KAN)-resistant haploid single deletion mutants were isogenic to SP286 (h+ ade6-M210 (M216);ura4-D18; leu1-32) and selected from the BIONEER haploid deletion collection (Kim et al., 2010) after being streaked from frozen stocks to single colonies. The nourseothricin (NAT) resistant *h*- query strains were made in 96-well format using the PEM2 strain (Roguev et al., 2007). Targeting cassettes were built using a 2-step, fusion PCR protocol in which long (3–3.5 kb) cassettes were amplified after annealing mediated by non-palindromic and unique GC-rich overlapping sequences (Fig S1). Specific integration of the NAT marker into the target locus was verified by failure to amplify the central 200-300 bases of the targeted gene and successful amplification of specific integration amplicons using primers upstream and downstream of the homologous recombination sequence paired with primers within the NATMX6 module. Query strains harboring constitutive hypomorphic Degron-DAmP alleles were made via the same strategy except the C-terminal degron sequence (Ravid and Hochstrasser, 2008) was fused in place of the stop codon, followed by the NATMX6 selectable maker in place of the 3'UTR. Mating, selection and propagation of the double mutants were carried on a Singer RoToR pinning robot using the PEM2 procedure (Roguev et al., 2008, 2007).

For directed assays in *S. cerevisiae* single and double mutations were generated *de novo* in WT W303 diploid cells, followed by sporulation and tetrad dissection. Individual spores were scored for their mendelian ratios and had their genotype confirmed by multiple PCR-based tests.

Genetic Interaction Score Acquisition and Analysis

Final double mutant plates were scanned on a flat-bed scanner (EPSON PhotoPerfection 350, Fig S2) and integrated colony intensities were extracted using a custom algorithm (scripts available

upon request) executed in MATLAB (The Mathworks, Natcik, MA). Subsequent analysis was performed as described, including normalization of plate surface artifacts, row/column normalization artifacts, and batch artifacts (Collins et al., 2010). Linkage biases due to the reduced frequency of recombination between linked loci (manifested by a reduced number of spores and a spurious negative S-score) were used to identify contaminated or mis-annotated strains (Fig S2D). For appropriately linked strains, spuriously low S-scores were removed from the dataset for loci within 300kb from each other. For loci between 300 and 600kb from each other, the relationship between distance and S-score was modeled per locus and query and array strains and spurious negative S-scores were normalized (Fig S2E, scripts available upon request).

Quantitative Reverse Transcriptase PCR (qRT-PCR).

Total RNA was isolated from 15 ml of mid-log phase *S. pombe* cultures via hot acid phenol extraction. Total RNA was DNAase treated, re-extracted with Phenol/Chloroform, and re-suspended at 500ng/ul and 4µg of RNA was used to make random hexamer primed cDNA with the SuperScript III First-Strand Synthesis System for RT-PCR (Invitrogen). Total RNA from siRNA transfected HeLa cells from 6-well plates were lysed and harvested and total RNA was isolated using the RNeasy Mini Kit (Qiagen). 1µg of total RNA was used to make oligo(dT) primed cDNA with the SuperScript III First-Strand Synthesis System for RT-PCR (Invitrogen). qPCR on the cDNAs was performed on the Light Cycler 480 II (Roche) using Light Cycler 480 Sybr Green I Master Mix (Roche). qPCR was performed with the following oligo pairs:

bip1: Fwd TCTCCTGCCCCTCGTGGTG; Rev TCGGCCTCCTTAACCATGCGC; 179 bp amplicon

rpl1901 Fwd AAGACCCATGCCGCCAAGCG; Rev GCAAAACACGTTGACGGCGCA; 115 bp amplicon

pgk1 Fwd GCTGACGCTTCTGCCGTCGA; Rev GGGACGAGCGGGGTTCTCCA;195 bp amplicon

STRN3 Fwd TGCTTCTGAGGACCATACCC; Rev GCCATCTGCTGAACAAGACA ; 334 bp amplicon

SLMAP Fwd CCCATGGGTGTATTGTTTCC; Rev CCGATGTAAGGCCTCCTGTA; 185 bp amplicon

STRIP1 Fwd AGGCAGTGACACGAACACAG; Rev GTTTCTGCAGGGACTTGCTC; 177 bp amplicon

MOBKL3 Fwd AGGCCAAGATGAAGGTGTGT; Rev AGACATGCAGCACCATCAAG, 219 bp amplicon

RPL19 Fwd ATGTATCACAGCCTGTACCTG; Rev TTCTTGGTCTCTTCCTCCTTG; 233 bp amplicon

Cp values were converted to standard quantities using standard curves for all primer sets. Triplicate qPCR samples for each biological triplicate were normalized to RPL19 for human cells and rpl1901 for fission yeast cells and relative values are shown. PCR specificity was validated by both melting curves of amplicons and agarose gel electrophoresis to confirm amplicon size. Efficacy of siRNA to silence specific targets in HeLa cells is displayed as a normalized mRNA abundance compared to siLUC (control) transfected cells (Fig S6).

Human Cell Culture and Transfection

Plasmids and transfections. cDNAs for human SLMAP were derived from pCR-BluntII-TOPO-SLMAP (Open Biosystems) and from HeLa cell cDNA derived from oligo dT primed mRNA. Full length cDNA and truncations corresponding to amino acids 1-538 and 1-637 were isolated by PCR using a common 5' primer:

Fwd GCGCGCCGTACGGATGCCGTCAGCCTTGGCCATC

and 3' specific primers:

Full Length Rev GCGCGCGAATTCTCATGGAGAAGCTCTGGCCAG

538 Rev GCGCGCGAATTCTCAAACTTGATTTCGATAGGC

637 Rev GCGCGCGAATTCTCAAAAACTGTTTTGCAGACTTG.

PCR products were digested with BsiWI and EcoRI and ligated into pQCmCherryXIN (a gift from Wes Sundquist) such that all expression clones were N-terminally labeled with mCherry. Prior to amplification and transfection, positive clones were identified and confirmed by sequencing. For transfections, cells were plated at 30-50% confluence in 12-well or 24-well dishes onto fibronectin-coated coverslips. Plasmids were incubated with polyethyleneimine (PEI) at a ratio of 5:1 (mg:mg of PEI:plasmid) and subsequently added to cells for 24 hours. Following transfection, cells were either permeabilized in 0.1% triton X-100 or fixed in 2% formaldehyde and then permeabilized and

subsequently mounted with ProLong Gold containing DAPI (Invitrogen). HeLa cells were maintained in DMEM supplemented with 10% FCS. Lines expressing GFP-fusions were maintained in medium containing 400µg/ml G418. For immunofluorescence experiments, cells were seeded on coverslips coated with 10µg/ml fibronectin and transfected with siRNA oligos at 30% confluence. For FACS experiments, cells were seeded on plastic and transfected with siRNA oligos at 30-50% confluence.

siRNA Design & Transfection

Two unique duplexes of siRNA oligos were designed as described previously using the Dharmacon siDESIGN center:

STRN3_1 sense (NM_014574.3)	GCAAAAGGGACAAGAAAUAtt
STRN3_2 sense	GAAGUAGGUUAUACAGAUAtt
SLMAP_1 sense (NM_007159.2)	GGUUAGAAGUUAUGGGAAAtt
SLMAP_2 sense	GAGAAUACACGGAAAGUUAtt
STRIP_1 sense (NM_033088.2)	GAGAAGAGGAAGAGGAGAAtt
STRIP_2 sense	GGACUGAGCUGGAUACCAAtt
MOBKL3_1sense (NM_001100819)	CGUAGGAUUUACAGAAUAUtt
MOBKL3_2 sense	CCAGAUACUUGCACUCAAAtt

Both duplexes were tested for silencing efficacy and specificity for STRN3, SLMAP and STRIP1. Efficacy was assessed by phenotypes observed via immuno-fluorescence and DNA content analysis using flow cytometry. The specificity of SLMAP depletion was confirmed by western blotting using an anti-SLMAP antibody (clone 2A7, Novus Biologicals). As antibodies for STRN3, STRIP1 and MOBKL3 were either ineffective or unavailable, qRT-PCR was utilized to confirm target specificity. HeLa cells were seeded in 12-well or 6-well dishes and transfected with 20nM siRNA duplexes using Lipofectamine RNAiMAX (Invitrogen) per the manufacturer's protocol. Cells were subsequently harvested at 48, 60 and 72 hours for immunofluorescence or flow cytometry.

Flow Cytometry.

Mammalian cells: cells were harvested after trypsinization and resuspended in 300µl of 25µg/ml propidium iodide (PI), 250µg/ml RNaseA and 0.1% Triton X-100 in PBS for a minimum of 30 min at 25°C. Alternatively, prior to PI treatment, cells were fixed overnight at 4°C in 70% ethanol. 10,000 cells were analyzed with the FACSCanto II fluorescence-activated cell sorter (BD Bioscience). For all experiments duplicate FACS samples of triplicate biological replicates were analyzed.

Yeast cells: Cells were grown overnight in rich media to OD600 ~0.3-0.8 (log phase). 1 OD600 (~10^7cells) was pelleted at 2000rpm for 5 minutes and fixed in 1 ml ice-cold ethanol while vortexing and subsequently left on ice for 20 minutes. 300 µl fixed cells were washed with 50 mM sodium citrate and resuspended in 500 µl 50mM sodium citrate containing 100µg/ml RNase A and incubated for 2 hours at 37°C. An additional 500 µl 50mM sodium citrate containing 8 µg/ml PI was then added and 50,000 cells were analyzed for forward scatter (size, FSC), side scatter (shape, SSC) and DNA content with the FACSCanto II. For all experiments triplicate FACS samples of biological duplicates were analyzed and averaged.

Immunofluorescence.

siRNA-transfected HeLa cells or HeLa cells stably expressing STRN3-eGFP or STRIP1-eGFP were fixed with 4% formaldehyde (10 min, 25°C for samples expressing GFP or stained with giantin antibodies (rabbit polyclonal, Covance)) or 100% ice-cold methanol (10 min, 25°C, pericentrin (rabbit polyclonal, Novus Biologicals) and anti-tubulin (mouse monoclonal, Sigma-Aldrich). Fixed cells were permeabilized with Triton-X100 (0.1%) or saponin (0.1% for samples stained with giantin antibodies) and incubated overnight at 4°C with primary antibodies in PBS containing 0.1% Triton X-100 and 3% BSA (PBST) or PBS containing 0.1% saponin and 1% BSA (PBSS). Cells were washed 3 times in PBS containing 0.1% Triton X-100 or 0.1% saponin and incubated in secondary antibodies conjugated to either Alexafluor488 or 594 (Invitrogen, Eugene, OR) diluted in PBST or PBSS for 1 hour. Cells were

washed 3 times with PBS containing 0.1% Triton X-100 or 0.1% saponin and cover slips were mounted with ProLong Gold antifade reagent with DAPI (Invitrogen). Alexafluor488, 594, DAPI and GFP signals were imaged on a 100x oil-immersion objective on an Axiovision microscope (Zeiss).

Western Blotting.

siRNA transfected HeLa cells from 6-well plates were lysed in RIPA (50mM Tris pH8, 150mM NaCl, 1.0% Triton X-100, 0.5% Na-deoxycholate, 0.1% SDS and complete protease inhibitor tablet (Roche)). 20µg of whole cell lysate was electrophoresed on 4-20% gradient acrylamide gel and transferred to nitrocellulose membranes. Membranes were blocked with 5% non-fat dry milk in tris-buffered saline and 0.05% Tween20 (TBST) (50mM Tris pH 7.6, 150mM NaCl, 0.05% Tween 20) and incubated with primary antibodies to SLMAP (mouse monoclonal, Novus Biologicals) and anti-tubulin (mouse monoclonal, Sigma-Aldrich) overnight at 4°C. After washing with TBST, membranes were incubated with IRDye 800 CW goat anti mouse secondary antibodies (1:10000, Li-Cor) in TBST with 0.01% SDS for 45 min at 25°C. Membranes were subsequently washed with TBST and TBS and fluorescence was analyzed on the Odyssey Imager (Li-Cor).

Affinity-Purification & Mass Spectrometry

HeLa STRN3-eGFP and STRIP1-eGFP cells were generated as described (Poser et al., 2008). HeLa STRN3-eGFP and untagged HeLa cells were cultured in standard cell culture conditions, expanded to 3 x 15cm cell culture dishes in triplicate experiments, harvested with Trypsin and flash frozen in liquid nitrogen. Cells were lysed with 1ml per plate of 1.5% Digitonin containing IP buffer (50mM Hepes-KOH, 150mM KOAc, 2mM MgOAc, 1mM CaCl2, 15% glycerol, protease inhibitor). After a 45 min incubation step the cell lysate was clarified by a ultracentrifugation spin at 20min, 58,000g, 4°C. The supernatant was incubated with a 10µl bed volume of anti-GFP-antibody coupled agarose beads (trapA beads, Chromotek) for 1h at 4°C. The beads were then washed five times with

10ml of wash buffer I (0.1% Digitonin, 50mM Hepes-KOH, 150mM KOAc, 2mM MgOAc, 1mM CaCl2, 15% glycerol), washed once with 10ml of wash buffer II (50mM Hepes-KOH, 150mM KOAc, 2mM MgOAc, 1mM CaCl2, 15% glycerol) and once with 1ml of wash buffer II for transfer of the beads to 1ml snap lid tubes. Proteins recovered by the immunoaffinity purification were Trypsin digested on the agarose beads and peptides eluted and treated as previously described (Hubner et al., 2010).

Resulting peptides were subjected to reverse phase liquid chromatography on a Proxeon easy-nLC system (Thermo Fisher) and directly sprayed into an LTQ-Orbitrap mass spectrometer (Thermo Fisher). Raw files were processed with MaxQuant, version 1.2.0.22 (Cox and Mann, 2008), using the label free protein quantification algorithm and matching of peptide identifications between runs. Significant interactors were determined by comparing protein intensities in STRN3 and control immunoprecipitations and calculating t-test statistics. The cutoff criteria were based on a combination of fold change and p-value and were calculated using a permutation based method for a given false discovery rate as described (Hubner et al., 2010). Volcano plots were generated using the software R.

SUPPLEMENTAL CITATIONS

Altschul, S. F., Madden, T. L., Schäffer, A. A., Zhang, J., Zhang, Z., Miller, W., and Lipman, D. J. (1997). Gapped BLAST and PSI-BLAST: a new generation of protein database search programs. Nucleic Acids Res. *25*, 3389-3402.

Bullitt, E., Rout, M. P., Kilmartin, J. V., and Akey, C. W. (1997). The Yeast Spindle Pole Body Is Assembled around a Central Crystal of Spc42p. Cell *89*, 1077-1086.

Dujon, B., Sherman, D., Fischer, G., Durrens, P., Casaregola, S., Lafontaine, I., De Montigny, J., Marck, C., Neuvéglise, C., Talla, E., et al. (2004). Genome evolution in yeasts. Nature *430*, 35-44.

Cox, J., and Mann, M. (2008). MaxQuant enables high peptide identification rates, individualized p.p.b.-range mass accuracies and proteome-wide protein quantification. Nat. Biotechnol *26*, 1367-1372.

Eisen, M. B., Spellman, P. T., Brown, P. O., and Botstein, D. (1998). Cluster analysis and display of genome-wide expression patterns. Proc. Natl. Acad. Sci. U.S.A. *95*, 14863-14868.

Fitzpatrick, D. A., Logue, M. E., Stajich, J. E., and Butler, G. (2006). A fungal phylogeny based on 42 complete genomes derived from supertree and combined gene analysis. BMC Evol. Biol. *6*, 99.

Gordon, J. L., Byrne, K. P., and Wolfe, K. H. (2009). Additions, losses, and rearrangements on the evolutionary route from a reconstructed ancestor to the modern Saccharomyces cerevisiae genome. PLoS Genet. *5*, e1000485.

de Hoon, M. J. L., Imoto, S., Nolan, J., and Miyano, S. (2004). Open source clustering software. Bioinformatics *20*, 1453-1454.

Hubner, N. C., Bird, A. W., Cox, J., Splettstoesser, B., Bandilla, P., Poser, I., Hyman, A., and Mann, M. (2010). Quantitative proteomics combined with BAC TransgeneOmics reveals in vivo protein interactions. J. Cell Biol *189*, 739-754.

Kim, D.-U., Hayles, J., Kim, D., Wood, V., Park, H.-O., Won, M., Yoo, H.-S., Duhig, T., Nam, M., Palmer, G., et al. (2010). Analysis of a genome-wide set of gene deletions in the fission yeast Schizosaccharomyces pombe. Nat. Biotechnol *28*, 617-623.

Ravid, T., and Hochstrasser, M. (2008). Diversity of degradation signals in the ubiquitin-proteasome system. Nat Rev Mol Cell Biol *9*, 679-689.

Roguev, A., Bandyopadhyay, S., Zofall, M., Zhang, K., Fischer, T., Collins, S. R., Qu, H., Shales, M., Park, H. O., Hayles, J., et al. (2008). Conservation and rewiring of functional modules revealed by an epistasis map in fission yeast. Science *322*, 405.

Supplemental Figure1

Frost, A. *et al.*

Supplemental Figure 1

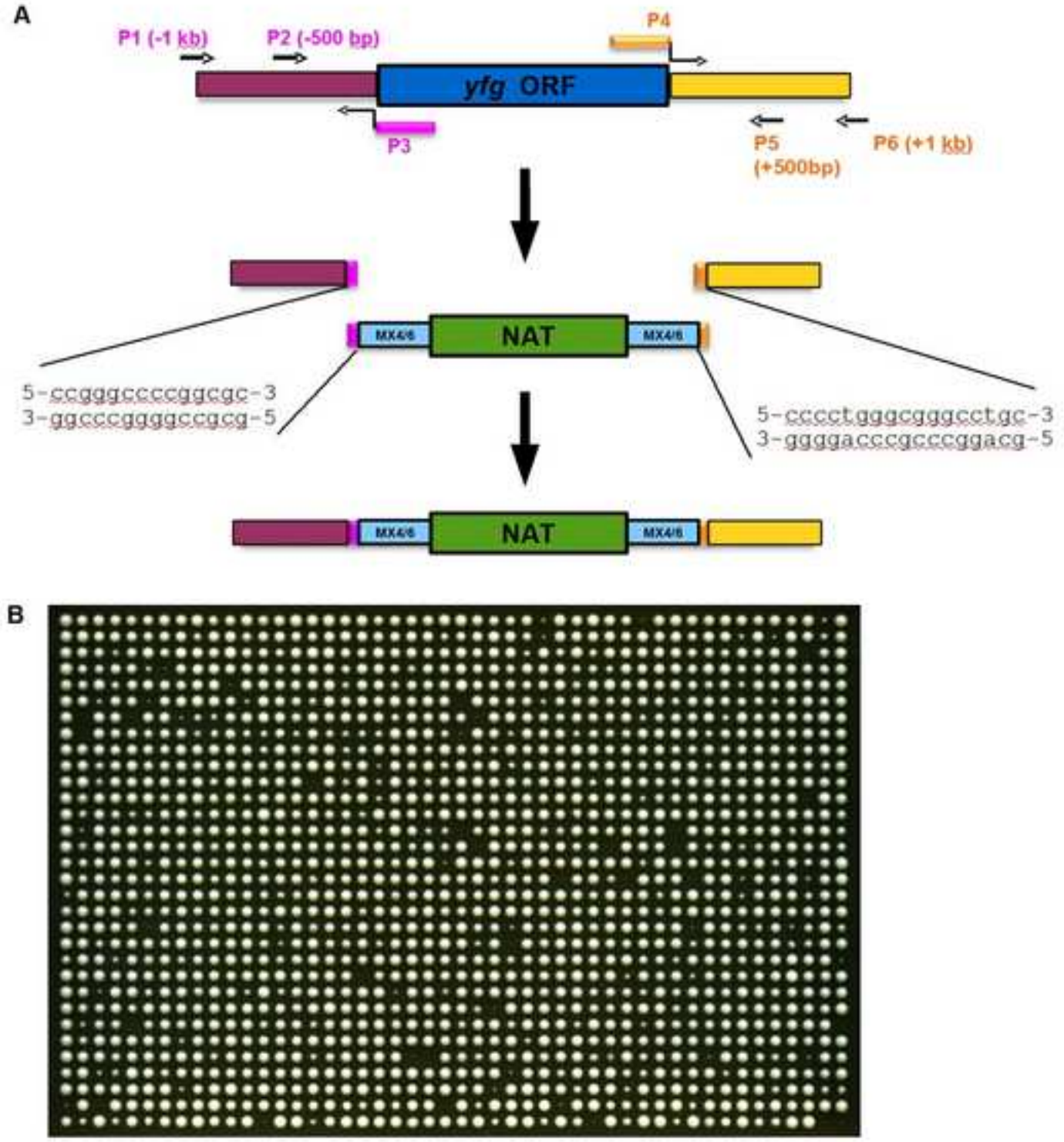

Supplemental Figure2

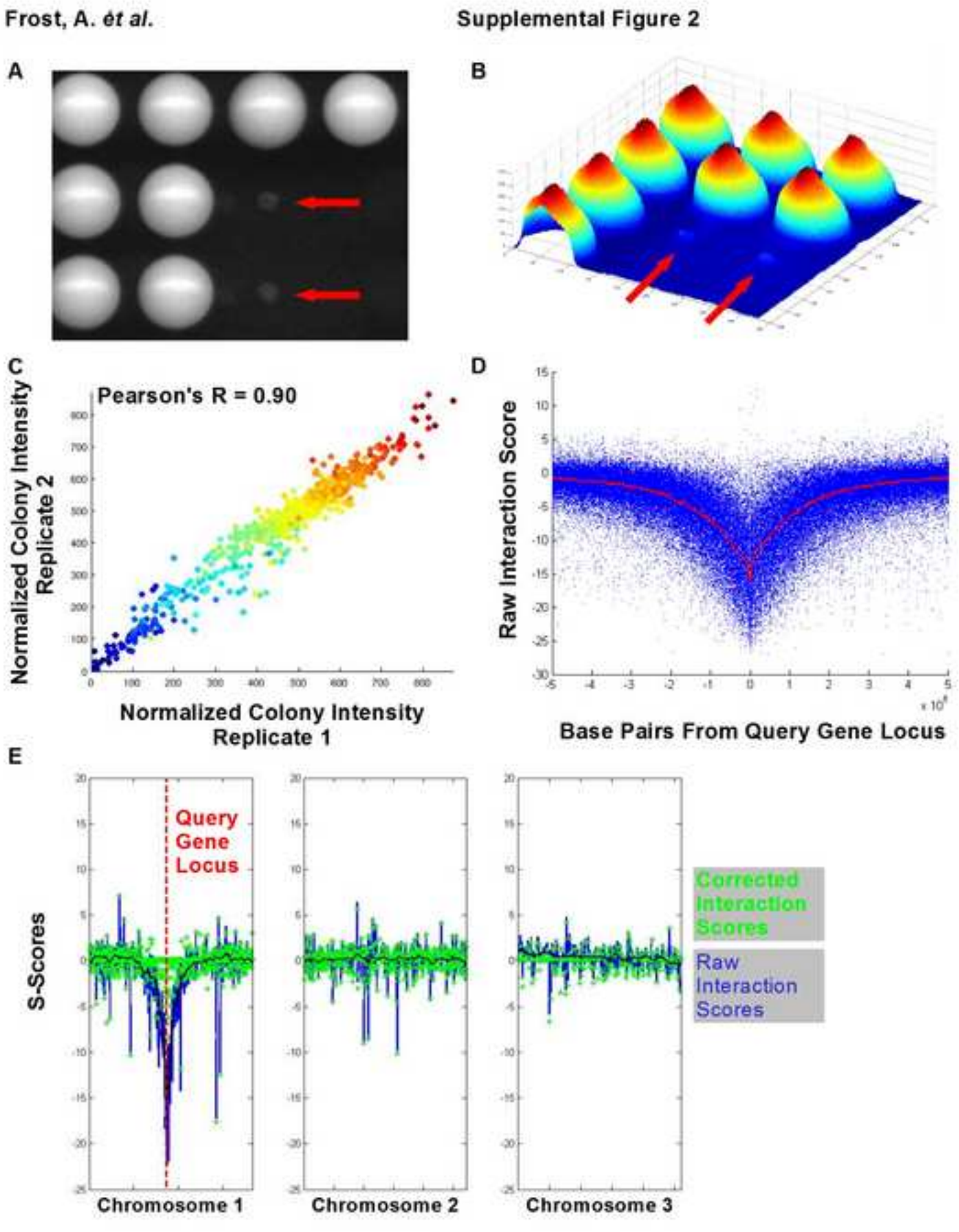

Supplemental Figure3

Frost, A. *et al.*

Supplemental Figure 3

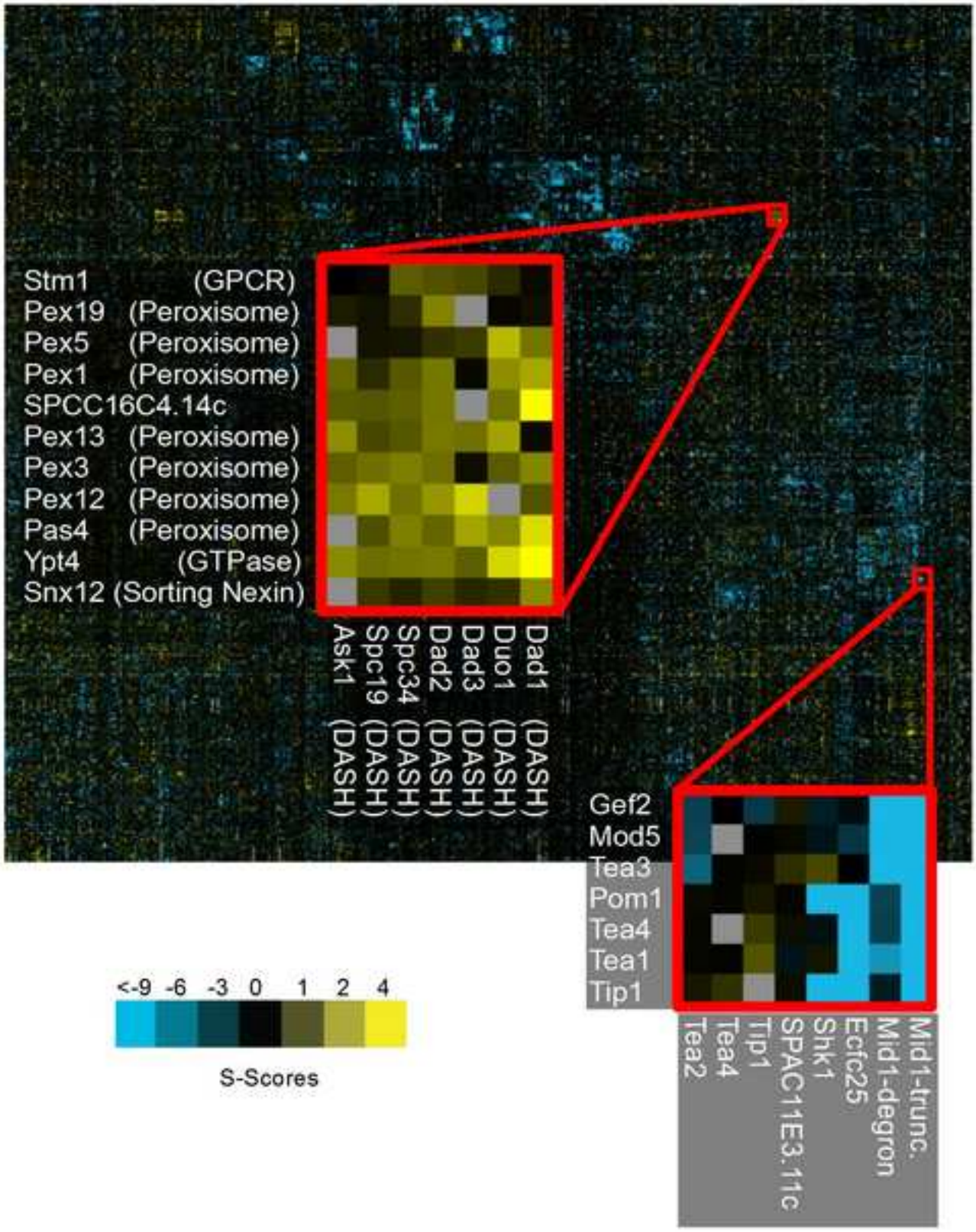

Supplemental Figure4

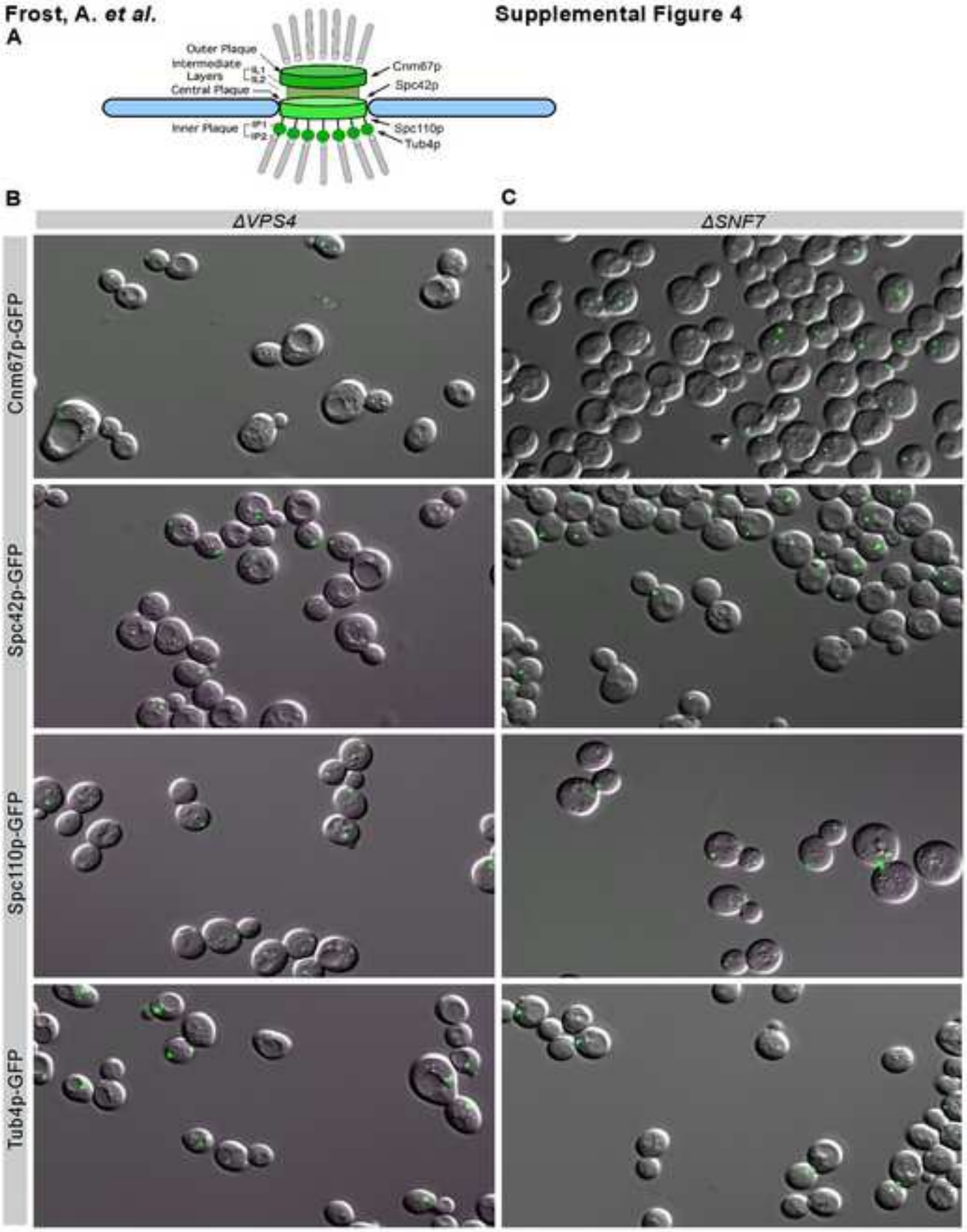

Frost, A. *et al.*

Supplemental Figure 5

A

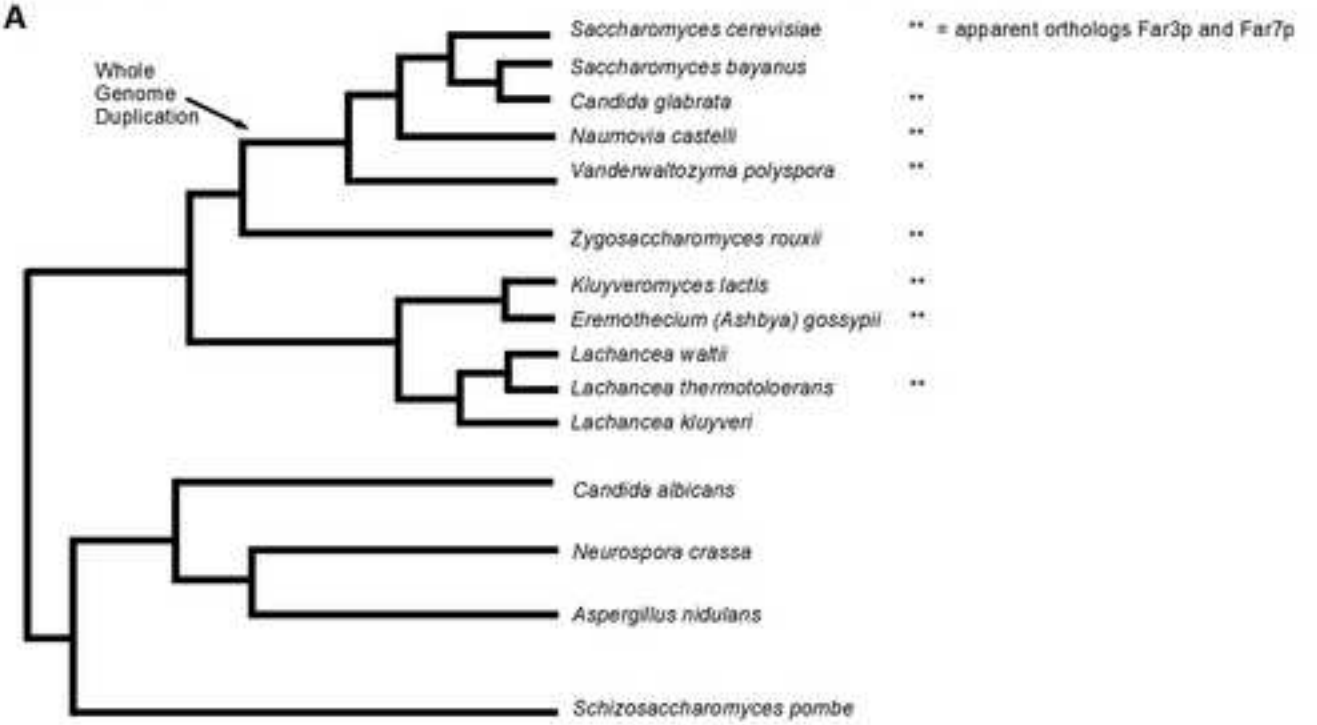

B

Amino acid sequences with significant Far3p alignments E-Values < 0.001:

gi	Name	Organism	Score(Bits)	E-Value
254582565	ZYRO0E01540p	*Zygosaccharomyces rouxii*	186	3e-57
343767032	NDAI_0A08700	*Naumovozyma dairenensis*	179	9e-55
255711374	KLTH0B04224p	*Lachancea thermotolerans*	174	9e-53
356890639	Ecym_5434	*Eremothecium cymbalariae*	172	6e-52
119873853	ADR125Wp	*Ashbya gossypii*	172	7e-52
50293155	hypothetical	*Candida glabrata*	169	6e-51
50312457	hypothetical	*Kluyveromyces lactis*	170	7e-51
342303903	NCAS_0I00180	*Naumovozyma castellii*	161	2e-47
156839806	Kpol_1073p20	*Vanderwaltozyma polyspora*	157	8e-46
344234403	CANTEDRAFT_112860	*Candida tenuis*	113	9e-29
354543648	CPAR2_104070	*Candida parapsilosis*	115	6e-27
164429322	hypothetical	*Neurospora crassa*	68	5e-04

Amino acid sequences with significant Far7p alignments E-Values < 0.001:

gi	Name	Organism	Score(Bits)	E-Value
255718971	KLTH0G16874p	*Lachancea thermotolerans*	195	2e-60
356890971	Ecym_6125	*Eremothecium cymbalariae*	191	3e-59
254583664	ZYRO0F04664p	*Zygosaccharomyces rouxii*	188	2e-57
302307809	AEL293Cp	*Ashbya gossypii*	181	1e-55
50287287	hypothetical	*Candida glabrata*	181	1e-54
342299664	NCAS_0A08620	*Naumovozyma castellii*	176	4e-53
50302393	hypothetical	*Kluyveromyces lactis*	173	5e-52
343770074	NDAI_0G02820	*Naumovozyma dairenensis*	169	5e-50
156839320	Kpol_467p6	*Vanderwaltozyma polyspora*	146	3e-41
254571251	hypothetical	*Komagataella pastoris*	123	4e-32
164425647	NCU06067	*Neurospora crassa*	32.7	3e-04
238878924	hypothetical	*Candida albicans*	32.3	5e-04

Supplemental Figure6